Experimental Determination of Zinc Isotope Fractionation in Complexes with the Phytosiderophore 2′-Deoxymugeneic Acid (DMA) and Its Structural Analogues, and Implications for Plant Uptake Mechanisms

Tamara Marković,[⊥] Saba Manzoor,[⊥] Emma Humphreys-Williams,[†] Guy JD Kirk,[‡] Ramon Vilar,[§] and Dominik J Weiss*[,⊥,‖]

[⊥]Department of Earth Science and Engineering, Imperial College London, London SW7 2AZ, United Kingdom
[†]Core Research Laboratory, Natural History Museum London, SW7 5BD, London, United Kingdom
[‡]School of Water, Energy & Environment, Cranfield University, Cranfield, Bedford MK43 0AL, United Kingdom
[§]Department of Chemistry, Imperial College London, London SW7 2AZ, United Kingdom
[‖]Stanford School for Earth, Energy and Environmental Sciences, Stanford University, Stanford California 94305, United States

Ⓢ *Supporting Information*

ABSTRACT: The stable isotope signatures of zinc and other metals are increasingly used to study plant and soil processes. Complexation with phytosiderophores is a key reaction and understanding the controls of isotope fractionation is central to such studies. Here, we investigated isotope fractionation during complexation of Zn^{2+} with the phytosiderophore 2′-deoxymugeneic acid (DMA), and with three commercially available structural analogues of DMA: EDTA, TmDTA, and CyDTA. We used ion exchange chromatography to separate free and complexed zinc, and identified appropriate cation exchange resins for the individual systems. These were Chelex-100 for EDTA and CyDTA, Amberlite CG50 for TmDTA and Amberlite IR120 for DMA. With all the ligands we found

preferential partitioning of isotopically heavy zinc in the complexed form, and the extent of fractionation was independent of the Zn:ligand ratio used, indicating isotopic equilibrium and that the results were not significantly affected by artifacts during separation. The fractionations (in ‰) were $+0.33 \pm 0.07$ (1σ, $n = 3$), $+0.45 \pm 0.02$ (1σ, $n = 2$), $+0.62 \pm 0.05$ (1σ, $n = 3$) and $+0.30 \pm 0.07$ (1σ, $n = 4$) for EDTA, TmDTA, CyDTA, and DMA, respectively. Despite the similarity in Zn-coordinating donor groups, the fractionation factors are significantly different and extent of fractionation seems proportional to the complexation stability constant. The extent of fractionation with DMA agreed with observed fractionations in zinc uptake by paddy rice in field experiments, supporting the possible involvement of DMA in zinc uptake by rice.
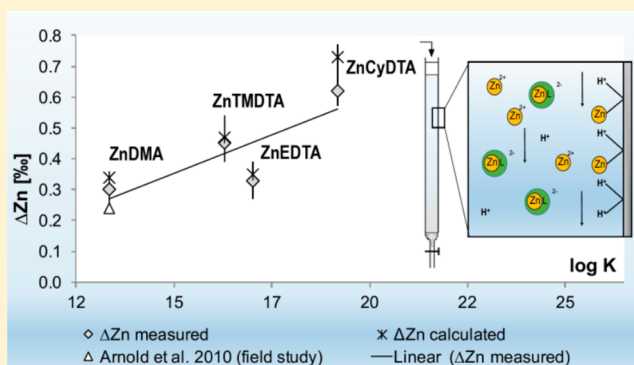
INTRODUCTION

With the introduction of multicollector inductively coupled plasma mass spectrometry (MC-ICP-MS), it has become possible to measure stable-isotope fractionation of metals in natural systems in the way that is routinely done for light elements such as C, O, N, and S.[1] Isotope systems are now available to study biogeochemical processes controlling trace element cycling in the natural environment. Of special interest are applications to study metal cycling in soil environments and during plant uptake, as mediated by rhizosphere processes. To date, complex root-soil interactions have only been studied indirectly using experiments in artificial laboratory systems or using mathematical modeling. The lack of direct techniques without artificial manipulations has hampered progress. Isotope fractionation at natural abundance has much to offer in this. Recent work has shown significant isotope fractionations in

trace element uptake by plants, as well as differences between plant species, likely reflecting different uptake mechanisms.[2]

In previous work on zinc uptake in rice, we found a light isotope bias in experiments conducted with solution cultures[3] but a neutral or heavy isotope bias in zinc uptake by rice grown in soils under aerobic and anaerobic conditions and with different zinc status.[4,5] This is suggesting that uptake mechanisms in rice are controlled by environmental factors. Indeed, studies with other plant types (hyper-accumulators and non-accumulators, grasses, trees) showed equally a neutral or heavy isotope bias during zinc uptake when grown in soils[6−9]

(a)

R₁=H, R₂=OH; Mugineic acid (1)

R₁= R₂=H; 2-Deoxymugineic acid (2)

R₁= R₂=OH; 3-Hydroxymugineic acid (3)

Phytosiderophores (PS) from the Mugineic acid family
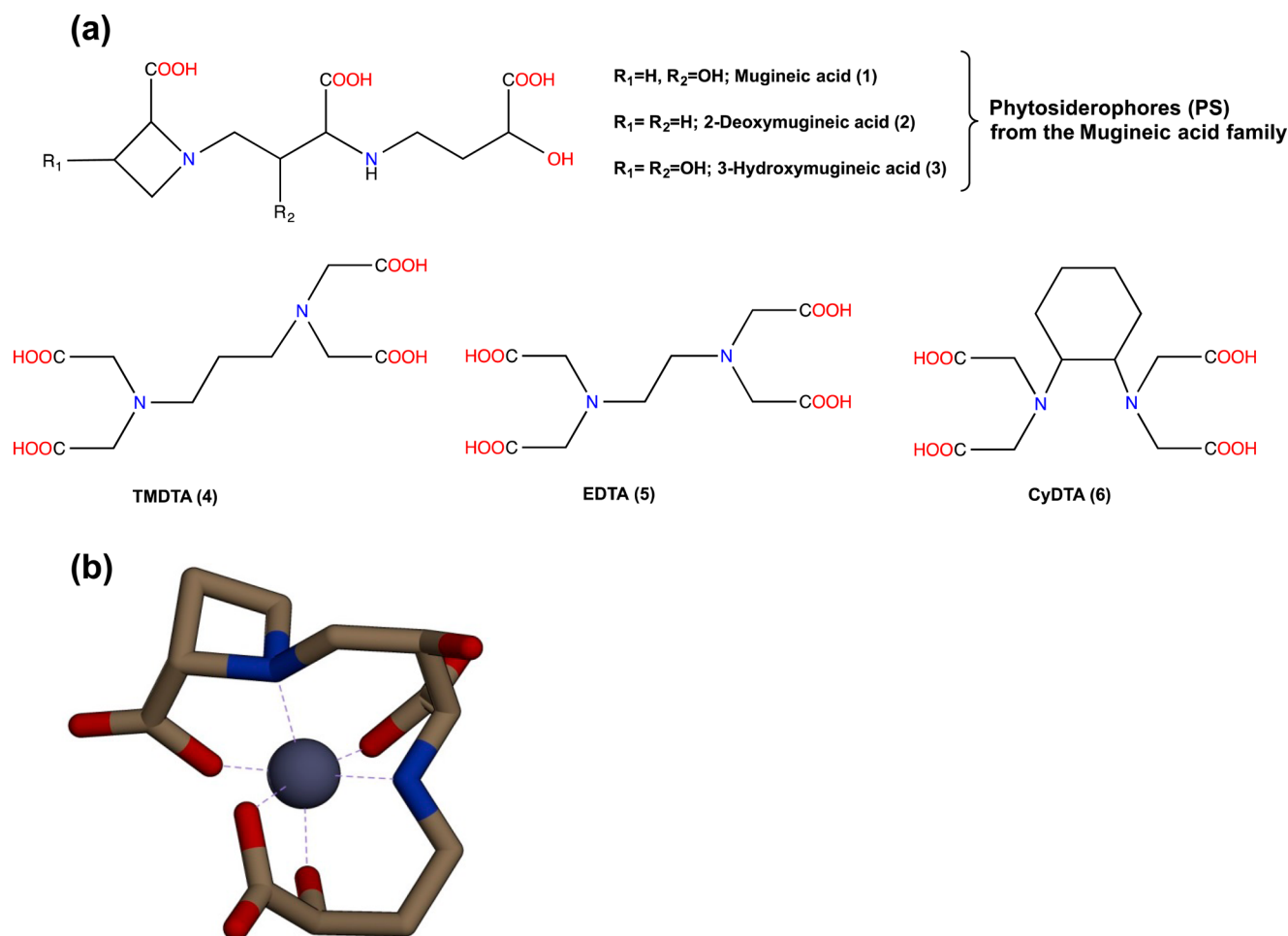
TMDTA (4)   EDTA (5)   CyDTA (6)

(b)

Figure 1. (a) Chemical structures of the four organic ligands tested in this study (2, 4−6), including a natural phytosiderophore-ligand from the family of mugineic acids. (b) Molecular structure of the Zn-MA complex modeled with molecular mechanics using ChemBio3D. Note that the color structures refer to Zn (iris, central atom), O (red) and N (blue). TmDTA, EDTA, and CyDTA coordinate to Zn(II) in an analogous fashion: via the two nitrogen atoms and the four carboxylate groups to give an octahedral complex.

and a light isotope bias in studies when grown in hydroponic solutions.[10−12]

Different processes have been proposed to explain the observed isotope patterns including zinc uptake from different soil pools[6] and the involvement of Zn-chelating phytosiderophores. The latter mechanism has been invoked because a heavy bias is expected in equilibrium fractionation during ligand formation.[13] Indeed, Guelke and von Blankenburg (2007) found a heavy isotope bias in iron uptake by grass species, which are known to secrete phytosiderophores to facilitate iron uptake; but a light isotope bias in iron uptake by non-grass species, which do not secrete phytosiderophores.[14]

It has been speculated that phytosiderophores are involved in the solubilization and uptake of soil zinc by rice, as well as in its transport within the plant.[4,15−17] To assess if observed isotope patterns in rice are possibly linked to Zn-chelating phytosiderophores, there is a need to constrain the equilibrium isotope fractionation during the complexation of zinc with phytosiderophores. However, there are significant experimental and analytical challenges to this. First, the phytosiderophore studied needs to be in a very pure state to avoid interferences during complexation. Isolates from plants and root secretions are prone to impurities.[18] It is preferable to synthesize the phytosiderophore. Protocols for the multistep synthesis of the

phytosiderophore DMA have been reported,[19,20] making DMA a suitable model phytosiderophore to study zinc fractionation. Second, there is the considerable challenge of separating free and complexed species from aqueous solutions without inducing artificial isotope fractionation.[21,22] The only previous attempt to do this for isotope fractionation studies of Zn-organic ligand complexation used a Donnan membrane.[23] Use of Donnan membranes, however, is time-consuming, prone to blank contributions due to the numerous steps involved, and there are possible implication of slow dissociation of metals.[24] Ion exchange chromatography can avoid these problems if suitable resins can be found as successfully demonstrated for iron.[22] The ion-exchange properties of potential resins can be predicted from the protonation and complexation constants of the resin's hydro-soluble active groups in aqueous solution. However, sorption of divalent metal ions on resins does not take place through simple ion exchange, and so the separation of free and complexed species is not easily predictable from the resin's ion-exchange properties alone.[25] To determine equilibrium isotope fractionation, there should be no exchange of zinc between the complex and exchange resin. One widely used approach to test this is to determine the isotope fractionation between reactants and products using a range of metal:ligand ratios.[21,26,27] The net isotope fractionation must be independ-

Table 1. Protocol for the Two Different Ion Exchange Procedures Used during This Study[a]

ion exchange procedure	objective	resin	system studied	elution procedure	step	medium	volume mL
cation exchange	to separate free Zn^{2+} from complexed ZnL^{2-}	Chelex-100, Na^+ form, 200−400 mesh	Zn/ZnEDTA	cation exchange	resin loading	H_2O	1−2
			Zn/ZnCyDTA		cleaning	2 M HCl	5 × 2
					conditioning	H_2O	3 × 2
		Amberlite CG50, H form, 100−200 mesh	Zn/ZnTmDTA		equilibration	KMES buffer (pH 6.2)	3 × 2
					sample loading	H_2O	5 × 2 up to 10 × 2
					matrix elution	KMES buffer (pH 6.2)	2 × 2
		Amberlite IR120, H^+ form	Zn/ZnDMA			H_2O	3 × 2
					Zn^{2+} fraction	1 M HCl	5 × 2
					cleaning	1 M NaOH	2 × 2
						H_2O	3 × 2
anion exchange	to remove isobaric and non isobaric interferences	AG MP1, BioRad, Cfrom, 100−200 mesh		anion exchange	resin loading	0.5 M HNO_3	1−2
					cleaning	0.5 M HNO_3	5 × 6
					conditioning	H_2O	5 × 3
						6 M HCl	4 × 1
					sample loading	6 M HCl	1 × 1
					matrix elution	6 M HCl	3 × 3
						2 M HCl	2 × 3.5
					Zn elution	0.1 M HCl	2 × 3.5
					cleaning	0.5 M HNO_3	5 × 2
						H_2O	5 × 1

[a]The cation exchange procedure for the separation of free from complexed zinc used Chelex-100, Amberlite CG50 and Amberlite IR120. The anion exchange chromatography for the removal of spectral and non-spectral interferences derived from the Na-rich matrix for subsequent high precision isotope ratio measurements used AG-MP1.

ent of the metal:ligand ratio within analytical precision. Other methods include the use of isotope spikes[21,22] but these are prone to issues such as equilibration rates.

Given these challenges, experimental studies of isotope fractionation between metal cations and organic ligands are still limited. Jouvin and colleagues[23] investigated the isotopic fractionation during adsorption onto purified humic acid (PHA) and found that zinc bound to PHA was isotopically heavier than free Zn^{2+} ($\Delta^{66}Zn_{ZnPHA\text{-}freeZn2+} = 0.24 \pm 0.06$). The fractionation factor depended on the affinity of the sites and on the pH of the solution. Using humic acids to improve our understanding of the underlying physical-chemical controls of isotope fractionation, however, has the disadvantage that they are structurally poorly constrained and hence a systematic investigation of structural controls (i.e., numbers of donors such as nitrogen, oxygen, the effect of the denticity, ligand affinity etc.) is not possible. Experimental studies involving other transition metals were conducted with iron and desferrioxamine B (DFOB),[21,22] EDTA and oxalate[22] and with copper and insolubilized humic acid (IHA),[28] ethylendiaminetetraacetic acid (EDTA), nitrotriacetic acid (NTA), iminodiacetic acid (IDA) and DFOB.[29] These experimental studies found all a preference for the heavy isotope during complexation and structural controls including complexation strength and bond distances were put forward as possible controls.

The goal of the present study was to determine for the first time isotopic fractionation factors for zinc complexation by a natural phytosiderophore, i.e., DMA, and structurally similar polydentate ligands. We synthesized DMA using recently published methods, and we identified the best resins to separate free and complexed Zn^{2+} for the ligands under study. We then determined the direction and extent of isotopic fractionation during complexation at different Zn:ligand ratios, and tested for possible controls such as ligand affinity and bonding environment.

■ MATERIALS AND METHODS

Choice of Ligands. We chose DMA since it has been proposed to play a major role in zinc uptake in rice. Furthermore, it is possible to obtain pure samples of this material via previously reported synthetic protocols.[19,20] We chose ethylenediaminetetraacetic acid (EDTA), trimethylene-dinitrilotetraacetic acid (TmDTA) and cyclohexanediaminetetraacetic acid (CyDTA) as additional ligands because they are commercially available, hexadentate ligands (like DMA) that bind zinc with high affinities giving complexes with the same overall geometry and coordination sphere as DMA, i.e. all the complexes are octahedral and they all use the same donor atoms to coordinate zinc: 4 oxygens and 2 nitrogens (Figure 1).

Synthesis of DMA. We used synthesis protocols previously published.[19,20] Details are given in the Supporting Information.

All starting materials and reagents were purchased from commercial sources and used without further purification. The progress of the synthesis was monitored by ^{1}H NMR spectroscopy at 297 K in the solvent indicated, using a Bruker AC300 spectrometer. The spectra were calibrated with respect to tetra-methylsilane and the residual solvent peaks indicated in the relevant spectrum.

Choice of Resins. Three resins were assessed based on their suggested abilities to sequester free Zn^{2+} without interacting with the Zn-ligand complex. The resins were Chelex-100 (BioRad, Na^+ form, 100−200 mesh, containing carboxyl functional groups) for the complexes with EDTA and CyDTA,[30] Amberlite CG50 (Dow, H^+ form, 100−200 mesh, containing carboxyl functional groups) for the complexes with TmDTA,[25,30] and Amberlite IR120 (Alfa Aesar, H^+ form, containing sulfonic acid functional groups) for the complexes with DMA.[18]

Preparation of Solutions. All solutions were prepared in Teflon Savillex vials (Savillex, MN, USA). Acid solutions were prepared using 18 MΩ-grade Millipore water (Bedford, MA, USA) and AnalaR grade HCl (6 M) and HNO_3 (15.4 M), both subdistilled. Stock solutions were prepared as follows: 1 mM $Zn(OAc)_2$ at pH 6.2 by dissolving $Zn(OAc)_2$ dihydrate (0.11 g) in 500 mL of MQ H_2O; and 1 mM Na_4EDTA by dissolving Na_4EDTA dihydrate (0.095 g) in 250 mL of MQ H_2O and heating at 60 °C until complete dissolution. Similarly, 250 mL of 1 mM stock solutions of TmDTA (0.077 g) and CyDTA monohydrate (0.091 g) were prepared. Potassium 2-(N-morpholino)ethanesulfonic acid (KMES) buffer solution (0.5 M) was prepared by dissolving MES monohydrate (26.66 g) in 250 mL of Millipore H_2O and stirring at 60 °C until complete dissolution was achieved. The pH of the solution was adjusted to 6.2 by the addition of 3 M KOH aqueous solution. $Zn(OAc)_2 \cdot 2H_2O$, CyDTA monohydrate and TMDTA were purchased from Sigma-Aldrich, Na_4EDTA from Fisher Scientific and MES monohydrate from VWR.

Different ratios (mol:mol) of free Zn^{2+} to complexed ZnL^{2-} were prepared by adding 10 mL of 1 mM $Zn(OAc)_2$ to the corresponding volumes of 1 mM ligand solution. All reagents were prepared using 18.2 mΩ cm Millipore water. The solutions were buffered to pH 6.2 using 0.5 M KMES and equilibrated overnight before proceeding to the ion exchange separation. Although all weighing was done gravimetrically, some error in molar quantities is possible for the ligand compounds due to their hygroscopic character. We confirmed that complete complexation was reached upon mixing equimolar solutions of $Zn(OAc)_2$ and L^{4-} (where L^{4-} refers to the deprotonated ligand) at pH 6.2 using GEOCHEM-EZ software.[31]

Commercial solutions of Cu (ROMIL Ltd., Cambridge, UK) and Zn (ROMIL Ltd., Cambridge, UK) were used as dopant solution for instrumental mass bias correction and for quality control of the isotope measurement on the MC-ICP-MS, respectively.[32]

Ion Exchange Procedures. We adapted two previously published ion exchange protocols: a cation exchange procedure for the separation of free and complexed zinc[33] and an anion exchange procedure for the separation of zinc fractions from the Na-rich solution matrix for subsequent isotope ratio measurements.[34] The protocol of these procedures is shown in Table 1. All resins were prepared and cleaned according to the manufacturers' recommendations and loaded onto BioRad PolyPrep columns. In general, the resin was soaked in 100 mL

of Millipore H_2O per 5 g of resin, and then pipetted into BioRad Poly-Prep (Bio-Rad Laboratories, CA) columns (i.d. Eight mm). The resin was cleaned with 2 M HCl and equilibrated with 0.5 M KMES buffer (pH 6.2). The buffered samples were loaded on to the column. The Zn-ligand complex was collected straight away as the samples ran down the column. The resin was further equilibrated with the buffer to elute any remaining complexed zinc. Washing the column with 1 M HCl eluted all free Zn^{2+} initially exchanged with the resin matrix. After collecting both free and complexed zinc, the fractions were evaporated to dryness and refluxed in 15.6 M HNO_3 at 100 °C for 3 h prior to drying at 120 °C to remove the easily oxidizable organic ligand material. After final drying, the samples were redissolved in 0.3 M HNO_3 for concentration measurements.

All collected samples, containing free Zn^{2+} or digested Zn-ligand complex, were evaporated to dryness, refluxed in 5.8 M HCl, diluted in 1 mL of 5.8 M HCl and passed through PolyPrep columns containing 0.7 mL AG-MP1 resin (Bio-Rad, Cl^- form, 100−200 mesh) anion-exchange resin, before evaporation and reflux in 15.6 M HNO_3. Evaporated samples were redissolved in 0.5 M HNO_3. The fractions containing Zn-ligand complexes were dissolved in a mixture of 5 mL 15.6 M HNO_3 and 3 mL 30% (v/v) H_2O_2, and digested using a microwave oven (210 °C, 1.7 kPa, 90 min) to break down the organic matrix.[35] All experimental work associated with preparation of samples and ion exchange chromatography was carried out in Class 10 laminar flow hoods in a Class 1000 Clean Laboratory.

Zinc Concentration and Isotopic Composition Measurements. Zinc concentrations were determined using ICP-AES (Thermo iCap 6500 Duo, Thermo Scientific, UK). Zinc isotope ratios were measured using multi collector ICP-MS (Nu Plasma, Nu Instruments, UK) and are expressed using the conventional δ^{66}Zn notation (‰):

$$\delta^{66}Zn = ((^{66}Zn/^{64}Zn)_{sample}/(^{66}Zn/^{64}Zn)_{standard} - 1)$$
$$\times 1000 \tag{1}$$

The empirical external normalization method[32] was used to correct for instrumental mass bias and the measurements were bracketed with the in-house standard London Zn. Accuracy and precision of the isotope measurements were assessed by analyzing two single element solutions during each measurement session: IRMM 0072 and Romil Zn.[36] The results were $\delta^{66}Zn_{IRMM} - \delta_{66}Zn_{London} = -0.25 \pm 0.07$ ‰ (2 SD, $n = 6$) and $\delta^{66}Zn_{Romil} - \delta^{66}Zn_{London} = -9.00 \pm 0.06$ ‰ (2 SD, $n = 6$). These $\delta^{66}Zn$ values agree well with previously published values.[36]

For every ligand system tested, the $\delta^{66}Zn$ values of the initial solution (i.e., $Zn(OAc)_2$) and of the free and complexed zinc fractions were determined. To quantify the isotope effect caused by complexation of zinc with the test ligands, the isotopic fractionation was calculated as

$$\Delta^{66}Zn_{ZnL2--Zn2+} = \delta^{66}Zn_{ZnL2-} - \delta^{66}Zn_{Zn2+} \tag{2}$$

where L refers to the tested ligand.

The isotope value for the complexed zinc fraction was also calculated using mass balance constraints to test the integrity of the data as organic containing samples are well-known to be difficult for precise and accurate isotope ratio measurements:

Table 2. Separation of Free (Zn^{2+}) from Complexed (ZnL^{2-}) Zinc Using the Three Different Resins Chelex-100, Amberlite CG50 and Amberlite IR120[a]

ligand	logK	resin	before column	after column				dissociation of complex
			mol fraction targeted Zn^{2+}/Zn$_{total}$	total Zn added	ZnL^{2-}-fraction	Zn^{2+}-fraction	mol fraction effective Zn^{2+}/Zn$_{total}$	
				mg	mg	mg		
CyDTA	18.5	Chelex-100	1.00	0.580	0.000	0.580	1.00	
			0.50	0.580	0.289	0.291	0.50	no
			0.00	0.580	0.580	0.000	0.00	no
EDTA	16.4	Chelex-100	1.00	0.463	0.000	0.463	1.00	
			0.50	0.555	0.258	0.297	0.53	no
			0.00	0.530	0.518	0.013	0.02	no
TmDTA	15.6	Chelex-100	1.00	0.610	0.000	0.610	1.00	
			0.50	0.622	0.131	0.492	0.79	partial
			0.00	0.662	0.235	0.426	0.64	partial
		Amberlite CG50	0.50	0.380	0.168	0.212	0.56	no
			0.00	0.371	0.328	0.044	0.12	no
DMA	12.8	Amberlite CG50	0.50	0.266	0.010	0.256	0.96	full
			0.00	0.267	0.019	0.248	0.93	full
		Amberlite IR120	0.50	0.190	0.127	0.062	0.33	possible
			0.00	0.204	0.175	0.029	0.14	possible

[a]Shown are the affinity constant (logK) for the formation of the relevant complex, the mole fraction of free Zn/total Zn in solutions before and after the passage through the resin, the total amount of zinc loaded onto the resin and the amount of zinc eluted from the resin after passage through column.

$$\delta^{66}Zn_{system} = (\delta^{66}Zn_{Zn2+}f_{Zn2+}) + (\delta^{66}Zn_{ZnL2-}f_{ZnL2-})$$

(3)

where $\delta^{66}Zn_{system}$ is the isotope composition of the initial solution, $\delta^{66}Zn_{Zn2+}$ and $\delta^{66}Zn_{ZnL2-}$ are the isotope values of the free and of the complexed Zn fraction, respectively, and f_{Zn2+} and f_{ZnL2-} are the mole fractions of free and of complexed Zn fractions calculated as $f_x = m_{fraction}/m_{total}$.

■ RESULTS AND DISCUSSION

Separation of Free and Complexed Zinc Using Cation Exchange Chromatography. We confirmed using GEO-CHEM-EZ[31] that complete complexation was reached upon mixing equimolar solutions of Zn(OAc)$_2$ and L^{4-}, where L^{4-} refers to the deprotonated ligand at pH 6.2, and that no other complexes were formed. Table 2 shows the separation performance of the resins with respect to the different Zn^{2+}/ZnL^{2-} systems studied in this work. Chelex-100 shows quantitative recovery and separation within 5% of the prepared mole fractions of free Zn^{2+} and ZnEDTA^{2-} and ZnCyDTA^{2-} complexes. EDTA and CyDTA were the ligands used with the highest affinity for zinc(II), i.e. with logK = 16.4 and logK = 18.5, respectively.[37] In contrast, Chelex-100 is too strong for the ZnTmDTA^{2-} complex (logK = 15.6) and we observe partial dissociation of the complex leading to an increased mole fraction of Zn^{2+}/Zn$_{total}$ in the eluent (Table 2). However, we found good separation in line with the mole fractions prepared for free Zn^{2+} and ZnTmDTA^{2-} using Amberlite CG50. With respect to DMA (logK = 12.8), we found a slight difference between the initial molar fraction and the measured one (Table 2). Although all weighing was done gravimetrically, there is inevitably some variability in the molar quantities of DMA due to its hygroscopic character. Other possible processes which could affect the molar fractions for the Zn^{2+}/ZnDMA^{2-} in the starting solution are small shifts in pH, complexation with the resin or effects of the matrix.[25] The differences between targeted and real mole fractions, however, did not affect the isotope fractionation (see discussion below), suggesting that dissociation from the resin was not the controlling process.

Figure 2 shows the elution sequence of the Zn^{2+}/ZnCyDTA^{2-} system. The zinc complexes are eluted from the corresponding resin during the sample loading process in H$_2$O and the subsequent matrix elution step using KMES buffer, whereas free Zn^{2+} is retained and only eluted on addition of 1 M HCl. Figures 2a to 2c show the elution profiles for three samples of the Zn^{2+}/ZnCyDTA^{2-} system with different molar ratios of free Zn^{2+} to total Zn. With no free Zn^{2+}, the ZnL^{2-} complex is eluted instantly and no further zinc is recovered upon elution with 1 M HCl. For the 0.5 mole fraction of free Zn^{2+}, the complexed ZnL^{2-} fraction is eluted during the sample loading and buffer elution steps, while the free Zn^{2+} is eluted with 1 M HCl. Finally, for the solution with only free Zn^{2+}, no Zn^{2+} is eluted during the initial two steps (sample loading and matrix elution with the buffer solution, Table 2), whereas upon addition of 1 M HCl, elution of free Zn^{2+} was instantaneous, explaining the sharp peak after 24 mL following the change to the 1 M HCl solution (Figure 2a). Between 96 and 105% of the zinc was recovered in all test conducted and shown in Table 2.

Isotope Fractionation during Complexation Reactions. Table 3 shows the isotope ratios (expressed using the $\delta^{66}Zn$ notation) of the free Zn^{2+} fraction (experimentally determined) and of the complexed zinc fraction (experimentally determined and calculated based on mass balance, see eq 3) for the four different ligands (DMA, EDTA, CyDTA, TmDTA) systems and for different mole fractions. Also shown is the recovery of zinc, that is, zinc loaded onto the column vs zinc eluted. In general, we obtained a very good recovery in all of them. Only experiments where measured and calculated
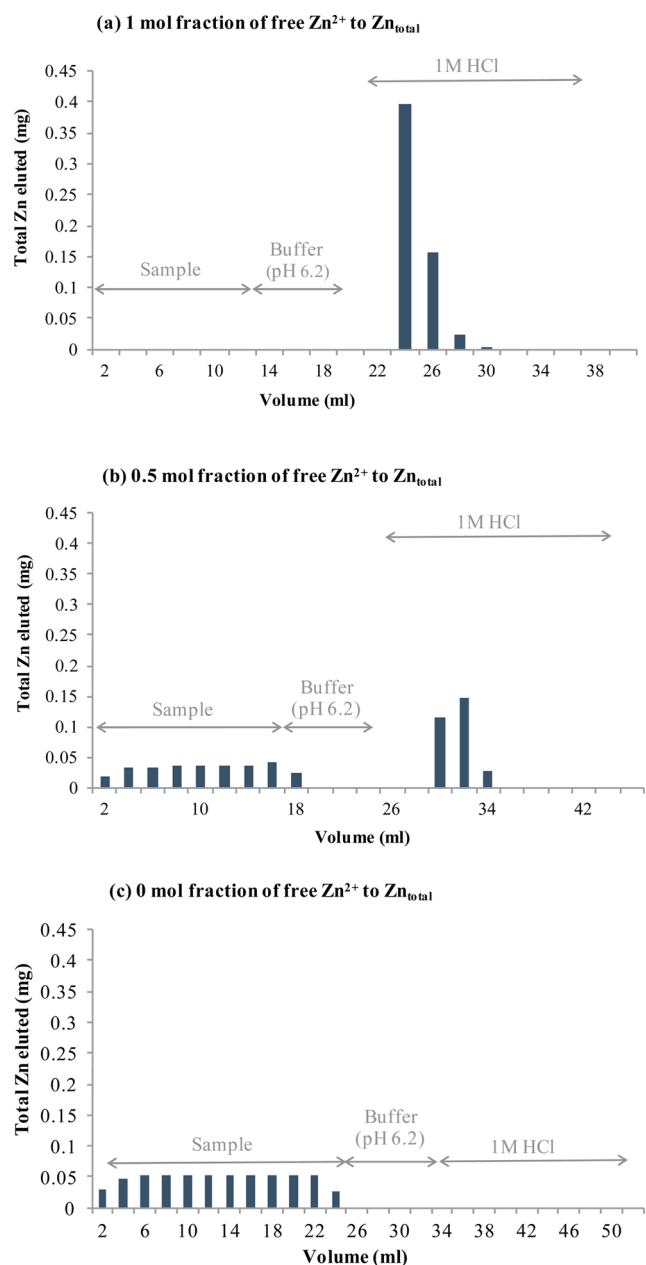
Figure 2. Elution profiles of solutions containing different mole fractions (i.e., 1, 0.5, 0) of free Zn^{2+} and complexed $ZnCyDTA^{2-}$ at pH 6.2 (buffered with 0.5 M KMES buffer). (a) 1 mole fraction of free Zn^{2+} to total Zn in the solution shows complete elution of Zn^{2+} in the presence of 1 M HCl. (b) 0.5 mole fraction of $ZnCyDTA^{2-}$ is eluted instantly with 0.5 M KMES whereas for eluting free Zn^{2+} fraction 1 M HCl is needed. (c) In 0 mole fraction sample all zinc is eluted instantly in the complexed form. No free Zn^{2+} is present, as visible from the elution profile after addition of 1 M HCl to the columns.

values for $\delta^{66}Zn_{ZnL2-}$ agreed within the reproducibility of the isotope ratio determinations were considered for further evaluation, guaranteeing an internally consistent data set.

As seen in Table 3, we found that the heavier isotope is preferred in the complexed zinc in all four ligand systems investigated during the course of this study (Table 3). The preferential accumulation of the heavy isotope in the ZnL^{2-} complexes is in agreement with equilibrium reaction dynamics on formation of strong bonds between metals and ligands.[13] The magnitude of isotope fractionation between free and

complexed zinc (expressed as $\Delta^{66}Zn_{ZnL2--Zn2+}$, eq 2) are within error for the different mol fractions studied in each system. Theory predicts that if a closed system is at isotopic equilibrium, then the Δ-value will be independent of the mol fraction.[38] The fractionation factors determined in this study are therefore at thermodynamic equilibrium. Dissociation of the ZnL^{2-} complex on the resins, including for the $Zn^{2+}/ZnDMA^{2-}$ system, is thus unlikely or at least insignificant as discussed above. The average values for $\Delta^{66}Zn_{ZnL2-Zn2+}$ are $+0.33 \pm 0.07$ ‰ (1σ, $n = 3$) for $ZnEDTA^{2-}$, $+ 0.45 \pm 0.02$ ‰ (1σ, $n = 2$) for $ZnTmDTA^{2-}$, $+ 0.62 \pm 0.05$ ‰ (1σ, $n = 3$) for $ZnCyDTA^{2-}$, and $+0.30 \pm 0.07$ ‰ (1σ, $n = 4$) for $ZnDMA^{2-}$.

Table 4 gives a compilation of selected fractionation factors normalized per atomic mas unit for the complexation of transition metals (Fe, Zn, Ni, and Co) with organic ligands derived from experimental and theoretical studies alike. We find that the experimentally determined fractionation factor for zinc complexation with humic acid[23] is smaller than that for zinc complexation with DMA and the other synthetic ligands studied in this study. Computationally determined fractionation factors for zinc complexation with citrate and malate, i.e., organic molecules smaller than the ligands studied in this study, show less positive or even negative fractionation.[39–41] Negative fractionation is also observed in computational studies of the complexation of citrate with Ni and Fe.[41] A recently published experimental study of copper complexation with natural and synthetic ligands[29] showed fractionation factors of similar magnitudes for EDTA and for CyDTA (Table 3). It is also noteworthy that the isotope fractionation of copper is (i) larger for the complexation with CyDTA than with EDTA and (ii) lower for the complexation with fulvic acid than with synthetic ligands. Both trends seem to hold for Zn (see Table 3 and Jouvin et al., 2009). For Fe, experimental and theoretical studies showed larger fractionation factors during complexation with phytosiderophores and synthetic ligands than with smaller organic ligands such as oxalate or citrate.[21,22,42] Table 4 also highlights the disagreement between previous experimental[21] and theoretical[43] studies on the sense of fractionation between Fe-desferrioxamine B (Fe-DFBO) and $Fe(H_2O)_6^{3+}$. Finally, the range of zinc isotope variation observed to date in the terrestrial environment is approximately $\Delta^{66}Zn \sim 1.8‰$[44] and therefore our data suggests that the extent of fractionation for zinc observed during complexation with phytosiderophores is significant and likely plays a major control of the global biogeochemical cycle of Zn isotopes.[45]

Controls of Isotope Fractionation. The results for the four hexadentate ligands allow us to explore the link between isotope signatures, reactivity and structure. Despite the similarity in Zn-coordinating donor groups, the differences in the exact geometries of the ZnL^{2-} complexes result in a range of affinity constants ($\log K$) between 12.8 and 18.5[37,46] and lead to significantly different isotope fractionation. Figure 3 shows the relationship between $\log K$ and the isotopic fractionation found in our study. There is strong evidence for an increase in heavy bias with increasing complexation strength. This trend has been inferred before by computational studies of organic and inorganic zinc complexes.[39] Similar conclusions were drawn in a theoretical study of organic and inorganic ligands using transition metals including iron, nickel, zinc, and copper.[41]

We obtain the relationship $\Delta^{66}Zn = (0.049 \pm 0.02) \times \log K - (0.366 \pm 0.390)$ ($r^2 = 0.67$, $p = 0.35$). A strong relationship between isotopic fractionation and $\log K$ with organic ligands

Table 3. Experimentally Determined δ^{66}Zn-Value for Free Zn^{2+} and for Complexed ZnL^{2-} Fractions in Solutions with Different Mole Fractions (Expressed as $f_{Zn} = Zn^{2+}/Zn_{total}$)[a]

ligand	sample ID	fractions: Zn^{2+} mass mg	mol fraction	δ^{66}Zn per mill	±2SD	ZnL^{2-} mass mg	mol fraction	δ^{66}Zn measured per mill	δ^{66}Zn calculated per mill	±2SD	Δ-value measured per mill	calculated per mill	n	mass balance: Zn added mg	Zn eluted mg	recovery %
EDTA	stock solution							−0.06								
	1	0.114	0.20	−0.33	0.07	0.47	0.80	nd	nd	0.01	nd	0.34		0.583	0.582	100
	2	0.488	1.00	0.04	0.03	0.000	0.00	nd	nd	nd	nd	nd		0.583	0.488	84
	3	0.157	0.27	−0.33	0.08	0.421	0.73	0.07	0.00	0.04	0.40	0.37		0.583	0.579	99
	4	0.249	0.43	−0.27	0.07	0.327	0.57	0.07	0.03	0.10	0.34	0.38		0.583	0.576	99
	5	0.398	0.70	−0.15	0.06	0.174	0.30	0.10	0.04	0.16	0.26	0.31		0.583	0.572	98
	6	0.564	1.00	−0.04	0.01	0.00	0.00	nd	nd	nd	nd	nd		0.583	0.564	97
	mean										**0.33**	**0.35**	**3**			
	±1SD										**0.07**	**0.04**				
TmDTA	stock solution							0.09								
	7	0.026	0.03	−0.31	0.05	0.774	0.97	0.12	0.07	0.10	0.43	0.41		0.739	0.800	108
	8	0.270	0.35	−0.25	0.11	0.505	0.65	0.21	0.18	0.27	0.46	0.53		0.739	0.775	105
	mean										**0.45**	**0.47**	**2**			
	±1SD										**0.02**	**0.08**				
CyDTA	stock solution							0.01								
	9	0.003	0.01	nd	nd	0.545	0.99	nd	nd	nd	nd	nd		0.583	0.548	94
	10	0.086	0.16	−0.50	0.16	0.453	0.84	0.06	0.01	0.11	0.57	0.61		0.583	0.539	92
	11	0.456	1.00	−0.01	0.1	0.000	0.00	nd	nd	nd	nd	nd		0.583	0.456	78
	12	0.002	0.00	nd	nd	0.613	1.00	−0.02	0.00	nd	nd	nd		0.583	0.615	105
	13	0.109	0.20	−0.62	0.02	0.437	0.80	0.04	0.02	0.17	0.66	0.79		0.583	0.546	94
	14	0.266	0.48	−0.40	0.02	0.283	0.52	0.23	0.00	0.39	0.62	0.79		0.583	0.550	94
	15	0.528	1.00	0.05	0.01	0.000	0.00	nd	nd	nd	nd	nd		0.583	0.528	91
	mean										**0.62**	**0.73**	**3**			
	±1SD										**0.05**	**0.10**				
DMA	stock solution							0.01								
	16	0.133	0.31	−0.23	0.07	0.300	0.69	0.13	0.01	0.12	0.36	0.34		0.414	0.434	105
	17	0.203	0.53	−0.16	0.06	0.179	0.47	0.07	0.03	0.21	0.24	0.37		0.414	0.382	92
	18	0.142	0.35	−0.21	0.01	0.258	0.65	0.15	0.06	0.13	0.36	0.34		0.414	0.400	97
	19	0.216	0.57	−0.12	0.09	0.165	0.43	0.13	0.03	0.18	0.26	0.31		0.414	0.381	92
	mean										**0.30**	**0.34**	**4**			
	±1SD										**0.07**	**0.03**				

[a]The δ^{66}Zn-value of the complexed ZnL^{2-} fraction was also calculated using mass balance constraints. (See text for details). The experimental fraction factor for the complexation of Zn^{2+} with ZnL^{2-} was calculated for each solution using $\Delta^{66}Zn = \delta^{66}Zn_{ZnL2} - \delta^{66}Zn_{Zn2+}$ and then averaged for each Zn^{2+}/ZnL^{2-} system using the available Δ^{66}Zn values (the mean is shown in bold, n indicates the number of Δ^{66}Zn values used, ± 1SD indicates the standard deviation). Also shown are recoveries of the ion exchange procedure and the amount of zinc loaded upon the resin and collected afterwards.

Table 4. Published Fractionation Factors of Transition Metals during Complexation with Organic Ligands Determined Experimentally and by Theoretical Calculations[a]

element	complexation reaction	isotope fractionation per mill per atomic mass unit	comment		reference
iron	$Fe^{3+} + DFOB^{4-} = [Fe(DFOB)]^-$	0.3	experimental	phase separation	Dideriksen et al., 2008
	$Fe^{3+} + DFOB^{4-} = [Fe(DFOB)]^-$	>0	experimental	membrane separation	Morgan et al., 2010
	$Fe^{3+} + DFOB^{4-} = [Fe(DFOB)]^-$	−0.2	ab initio calculations	DFT theory	Domagal-Goldman et al., 2009
	$Fe^{3+} + 2\ citrate^{3-} = [Fe(citrate)_2]^{3-}$	−0.4	ab initio calculations	DFT theory	Fujii et al. 2014
	$Fe^{2+} + citrate^{3-} = [Fe(citrate)_2]^{4-}$	−0.6	ab initio calculations	DFT theory	Fujii et al. 2014
	$Fe^{2+} + Nicotinamine^{4-} = [Fe(Nicotinamine)]^{2-}$	−0.03	ab initio calculations	DFT theory	Moynier et al., 2013
	$Fe^{3+} + Phytosiderophore^{3-} = [Fe(Phytosiderophore)]^0$	0.5	ab initio calculations	DFT theory	Moynier et al., 2013
zinc	$Zn^{2+} + PHA^{n-} = [Zn(PHA)]^{m-}$	0.1	experimental	membrane separation	Jouvin et al., 2009
	$Zn^{2+} + citrate^{3-} = [Zn(citrate)]^-$	0.07 to 0.25	ab initio calculations	DFT theory	Black et al., 2011
	$Zn^{2+} + [citrate(H_2O)_3]^{3-} = [Zn(citrate(H_2O)_3)]^-$	0.1	ab initio calculations	DFT theory	Fujii and Albarede, 2012
	$Zn^{2+} + citrate^{3-} = [Zn(citrate)_2]^{4-}$	−0.4	ab initio calculations	DFT theory	Fujii and Albarede, 2012
	$Zn^{2+} + [malate(H_2O)_4]^{2-} = [Zn(malate(H_2O)_4)]^0$	0.1	ab initio calculations	DFT theory	Fujii and Albarede, 2012
	$Zn^{2+} + [(malate)_2(H_2O)_2]^{4-} = [Zn(malate)(H_2O)_n]^{m-}$	−0.2	ab initio calculations	DFT theory	Fujii and Albarede, 2012
nickel	$Ni^{2+} + citrate^{3-} = [Fe(citrate)_2]^{4-}$	−0.6	ab initio calculations	DFT theory	Fujii et al. 2014
copper	$Cu^{2+} + IHA^{n-} = [Zn(IHA)]^{m-}$	0.1	experimental	membrane separation	Bigalke et al, 2010
	$Cu^{2+} + DFOB^{4-} = [Cu(DFOB)]^{2-}$	0.42	experimental	membrane separation	Ryan et al., 2014
	$Cu^{2+} + CyDTA^{4-} = [Cu(CyDTA)]^{2-}$	0.31	experimental	membrane separation	Ryan et al., 2014
	$Cu^{2+} + EDTA^{4-} = [Cu(EDTA)]^{2-}$	0.25	experimental	membrane separation	Ryan et al., 2014
	$Cu^{2+} + Nitrilotriacetic\ acid^{3-} = [Cu(Nitrilotriacetic\ acid)]^-$	0.22	experimental	separation	Ryan et al., 2014
	$Cu^{2+} + Fulvic\ acid^{\ n-} = [Cu(Fulvic\ acid)]^{m-}$	0.07	experimental	membrane separation	Ryan et al., 2014

[a]The fractionation is expressed using Δ-values in per mill per atomic mass unit, i.e., $\Delta^{x/y}M = (\delta^{x/y}ML^{2-} - \delta^{x/y}M^{2+})/(x\text{-}y)$, where x and y are two different isotopes (x = heavy and y = light), M is the metal studied and δ is the small delta value for free (M^{2+}) and complexed (ML^{2-}) species. DFBO = desferrioxamine B, PHA = purified humic acid, IHA = insolubilized humic acid, EDTA = ethylenediaminetetraacetic acid, TmDTA = trimethylenedinitrilotetraacetic acid, CyDTA = cyclohexanediaminetetraacetic acid.

has been suggested experimentally also for iron[22,47] and copper.[28,29] We note that the slope of the linear regression determined for zinc (0.049, this study) and for copper (0.036,[29]) are very similar. While the assessed linear relationship obtained in Figure 3 is affected by the lower value for the EDTA, it is worthwhile to note that the empirical equation predicts negative fractionations for smaller organic molecules such as oxalate, malate and citrate s predicted previously using calculations[41] (Table 4).

The positive correlation between complexation constant and isotope fractionation observed here may provide a simple empirical tool that may be used to predict fractionation factors for Zn-ligand complexes not yet studied experimentally but relevant to a wide range of biological, medical and environmental relevant ligands.

Comparison with Observed Isotope Fractionation of Zinc during Plant Uptake. Significant positive isotope fractionation has been observed for zinc uptake by rice grown in paddy soil.[4,5] The authors tentatively ascribed the heavy isotope bias to uptake of zinc complexed to DMA, consistent with a mathematical modeling exercise.[48] The extent of the heavy isotope fractionation we have determined upon zinc complexation by DMA matches the fractionation measure for soil-grown rice[4] as shown in Figure 3. Further work is needed
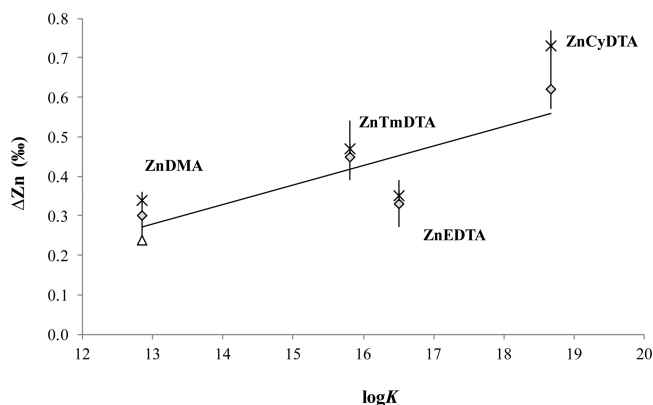
Figure 3. Measured and calculated isotopic fractionation of zinc upon complexation by the four organic ligands studied (EDTA, CyDTA, TmDTA, and DMA) as a function of the stability constants (logK) of the complex formation.[37,46] The linear regression is given as $y = 0.049 \pm 0.02\ x - 0.366 \pm 0.390$, $R^2 = 0.6766$, $p < 0.35$). Diamonds symbolize $\Delta^{66}Zn$ values determined using experimentally measured $\delta^{66}Zn$ for the ZnL^{2-} fraction, crosses symbolize $\Delta^{66}Zn$ values determined using calculated $\delta^{66}Zn$ for the ZnL^{2-} fraction using mass balance considerations. The triangle symbolize the $\Delta^{66}Zn$ values between rice stem and soil solution determined in field experiments in paddy field soils[4]

to confirm that rates of DMA secretion by rice under relevant conditions are sufficient to account for enhanced zinc uptake. Further evidence of heavy isotope discrimination during uptake of complexed metals by plants is provided for zinc uptake by tomatoes growing in zinc deficient soil,[49] by hyperaccumulators,[8,50] and for iron uptake by phytosiderophore-secreting grasses.[14] Whereas in field and hydroponic studies, Jouvin and co-worker found a light isotopic fractionation of between 0 and −1‰ in copper uptake by graminaceous and nongraminaceous plants, suggesting that uptake was not mediated by complexation.[12]

The findings presented here should make an important contribution to the emerging picture of isotopes as novel technique to study the cycling of zinc and other trace element in the plant−soil environment and to resolve key questions such as mechanisms of zinc uptake in plants.

ASSOCIATED CONTENT

S Supporting Information

The Supporting Information is available free of charge on the ACS Publications website at DOI: 10.1021/acs.est.6b00566.

    Further details on the synthesis and characterization of DMA ligand material (PDF)

AUTHOR INFORMATION

Corresponding Author
*Phone: +44 20 7594 6383; e-mail: d.weiss@imperial.ac.uk.

Notes
The authors declare no competing financial interest.

ACKNOWLEDGMENTS

REFERENCES

(1) Wiederhold, J. G. Metal stable isotope signatures as tracers in environmental geochemistry. *Environ. Sci. Technol.* **2015**, *49* (5), 2606−2624.

(2) von Blankenburg, F.; Von Wiren, N.; Guelke, M.; Weiss, D. J.; Bullen, T. D. Metal stable isotope fractionation by higher plants. *Elements* **2009**, *5* (6), 375−380.

(3) Weiss, D. J.; Mason, T. F. D.; Zhao, F. J.; Kirk, G. J. D.; Coles, B. J.; Horstwood, M. S. A. Isotopic discrimination of Zn in higher plants. *New Phytol.* **2005**, *165*, 703−710.

(4) Arnold, T.; Kirk, G. J. D.; Wissuwa, M.; Frei, M.; Zhao, F. J.; Weiss, D. J. Evidence for the mechanisms of zinc efficiency in rice using isotope discrimination. *Plant, Cell Environ.* **2010**, *33*, 370−381.

(5) Arnold, T.; Markovic, T.; Guy, K.; Schoenbachler, M.; Rehkamper, M.; Zhao, F.; Weiss, D. Iron and zinc isotope fractionation during uptake and translocation in rice (Oryza sativa) grown in oxic and anoxic soils. *C. R. Geosci.* **2015**, *347*, 397−404.

(6) Houben, D.; Sonnet, P.; Tricot, G.; Mattielli, N.; Couder, E.; Opfergelt, S. Impact of Root-Induced Mobilization of Zinc on Stable Zn Isotope Variation in the Soil−Plant System. *Environ. Sci. Technol.* **2014**, *48*, 7866−7873.

(7) Couder, E.; Mattielli, N.; Drouet, T.; Smolders, E.; Delvaux, B.; Iserentant, A.; Meeus, C.; Maerschalk, C.; Opfergelt, S.; Houben, D. 2015.., Transpiration flow controls Zn transport in Brassica napus and Lolium multiflorum under toxic levels as evidenced from isotopic fractionation. *C. R. Geosci.* **2015**, *347*, 386−396.

(8) Tang, Y.-T.; Cloquet, C.; Sterckeman, T.; Echevarria, G.; Carignan, J.; Qiu, R.-L.; Morel, J.-L. Fractionation of stable zinc isotopes in the field-grown zinc hyperaccumulator noccaea caerulescens and the zinc-tolerant plant silene vulgaris. *Environ. Sci. Technol.* **2012**, *46* (18), 9972−9979.

(9) Viers, J.; Oliva, P.; Nonell, A.; Gélabert, A.; Sonke, J. E.; Freydier, R.; Gainville, R.; Dupré, B. Evidence of Zn isotopic fractionation in a soil−plant system of a pristine tropical watershed (Nsimi, Cameroon). *Chem. Geol.* **2007**, *239*, 124−137.

(10) Aucour, A. M.; Pichat, S.; Macnair, M. R.; Oger, P. Fractionation of stable zinc isotopes in the zinc hyperaccumulator Arabidopsis halleri and nonaccumulator Arabidopsis petraea. *Environ. Sci. Technol.* **2011**, *45* (21), 9212−9217.

(11) Deng, T.; Cloquet, C.; Tang, Y.-T.; Sterckeman, T.; Echevarria, G.; Estrade, N.; Morel, J.-L.; Qiu, R.-L. Nickel and zinc isotope fractionation in hyperaccumulating and nonaccumulating plants. *Environ. Sci. Technol.* **2014**, *48*, 11926−11933.

(12) Jouvin, D.; Weiss, D. J.; Mason, T. F.; Bravin, M. N.; Louvat, P.; Zhao, F.; Ferec, F.; Hinsinger, P.; Benedetti, M. F. Stable isotopes of Cu and Zn in higher plants: evidence for Cu reduction at the root surface and two conceptual models for isotopic fractionation processes. *Environ. Sci. Technol.* **2012**, *46* (5), 2652−60.

(13) Bigeleisen, J.; Mayer, M. G. Calculation of equilibrium constants for isotopic exchange reactions. *J. Chem. Phys.* **1947**, *15*, 261−267.

(14) Guelke, M.; von Blankenburg, F. Fractionation of stable iron isotopes in higher plants. *Environ. Sci. Technol.* **2007**, *41* (6), 1896−1901.

(15) Suzuki, M.; Takahashi, M.; Tsukamoto, T.; S, W.; Matsuhashi, S. Y. J.; Kishimoto, N.; Kikuchi, S.; Nakanishi, H.; Mori, S.; Nishizawa, N. K. Biosynthesis and secretion of mugineic acid family phytosiderophore in zinc-deficient barley. *Plant J.* **2006**, *48*, 85−97.

(16) Suzuki, M.; Tsukamoto, T.; Inoue, H.; S, W.; Matsuhashi, S.; Takahashi, M.; Nakanishi, H.; Mori, S.; Nishizawa, N. K. Deoxymugeneic acid increases Zn translocation in Zn deficient rice plants. *Plant Mol. Biol.* **2008**, *66*, 609−617.

(17) Hacisalihoglu, G.; Kochian, L. V. How do some plants tolerate low levels of soil zinc? Mechanisms of zinc efficiency in crop plants. *New Phytol.* **2003**, *159* (2), 341−350.

(18) Tagaki, S. Naturally occuring iron compounds in oat and rice root washings: 1. Activity Measurement and Preliminary Characterization. *Soil Sci. Plant Nutr.* **1976**, *22* (4), 423−433.

(19) Namba, K.; Murata, Y.; Horikawa, M.; Iwashita, T.; Kusumoto, S. A practical synthesis of the phytosiderophore 2′-deoxymugineic acid: a key to the mechanistic study of iron acquisition by graminaceous plants. *Angew. Chem., Int. Ed.* **2007**, *46* (37), 7060−7063.

(20) Walter, M. R.; Artner, D.; Stanetty, C. Synthesis of [13C4]-labeled 2′-deoxymugineic acid. *J. Labelled Compd. Radiopharm.* **2014**, *57* (13), 710−714.

(21) Dideriksen, K.; Baker, J. A.; Stipp, S. L. S. Equilibrium Fe isotope fractionation between inorganic aqueous Fe(III) and the siderophore complex, Fe(III)-desferrioxamine B. *Earth Planet. Sci. Lett.* **2008**, *269*, 280−290.

(22) Morgan, J. L. L.; Wasylenki, L. E.; Nusester, J.; Anbar, A. D. Fe Isotope Fractionation during Equilibration of Fe-Organic Complexes. *Environ. Sci. Technol.* **2010**, *44*, 6095−6101.

(23) Jouvin, D.; Louvat, P.; Juillot, F.; Marechal, C.; Benedetti, M. Zinc isotopic fractionation: why organic matters. *Environ. Sci. Technol.* **2009**, *43*, 5747−5754.

(24) Weng, L.; Alonso Vega, F.; Van Riemsdijk, W. Strategies in the application of the Donnan membrane technique. *Environ. Chem.* **2011**, *8* (5), 466−474.

(25) Pesavento, M.; Biesuz, R.; Cortina, J. L. Sorption of metal ions on a weak acid cation exchange resin containing carboxalicgroups. *Anal. Chim. Acta* **1994**, *298* (2), 225−232.

(26) Criss, R. E. *Principles of Stable Isotope Distribution*; Oxford University Press: Oxford, 1999.

(27) Johnson, C. M.; Beard, B. L.; Albarède, F., Overview and General Concepts. In *Geochemistry of Non-Traditional Stable Isotopes*; Johnson, C. M.; Beard, B. L.; Albarède, F., Eds.; Mineralogical Society of America, 2004; Vol. 55, pp 1−22.

(28) Bigalke, M.; Weyer, S.; Wilcke, W. Copper isotope fractionation during complexation with insolubilized humic acid. *Environ. Sci. Technol.* **2010**, *44*, 5496−5502.

(29) Ryan, B. M. K.; Degryse, F.; Scheiderich, K.; McLaughiln, M. J. Copper Isotope Fractionation during Equilibrium with Natural and Sythetic Ligands. *Environ. Sci. Technol.* **2014**, *48*, 8620−8626.

(30) Bowles, K. C.; Apte, S. C.; Batley, G. E.; Hales, L. T.; Rogers, N. J. A rapid Chelex column method for the determination of metal speciation in natural waters. *Anal. Chim. Acta* **2006**, *558*, 237−245.

(31) Shaff, J. E.; Schultz, B. A.; Craft, E. J.; Clark, R. T.; Kochian, L. V. GEOCHEM-EZ: a chemical speciation program with greater power and flexibility. *Plant Soil* **2010**, *330*, 207−214.

(32) Peel, K.; Weiss, D. J.; Chapman, J.; Arnold, T.; Coles, B. J. A simple combined sample-standard bracketing and inter-element correction procedure for accurate and precise Zn and Cu isotope ratio measurements. *J. Anal. At. Spectrom.* **2007**, *22*, 1−8.

(33) Kingston, H. M.; Barnes, I. L.; Brady, T. J.; Rains, T. C.; Champ, M. A. Separation of eight transition elements from alkali and alkaline earth elements in estuarine and seawater with chelating resin and their determination by graphite furnace atomic absorption spectrometry. *Anal. Chem.* **1978**, *50*, 2064−2070.

(34) Dong, S.; Weiss, D. J.; Strekopytov, S.; Kreissig, K.; Sun, Y.; Baker, A. R.; Formenti, P. Stable isotope ratio measurements of Cu and Zn in mineral dust (bulk and size fractions) from the Taklimakan Desert and the Sahel and in aerosols from the eastern tropical North Atlantic Ocean. *Talanta* **2013**, *114*, 103−109.

(35) Arnold, T.; Schonbachler, M.; Rehkamper, M.; Dong, S.; Zhao, F. J.; Kirk, G. J.; Coles, B. J.; Weiss, D. J. Measurement of zinc stable isotope ratios in biogeochemical matrices by double-spike MC-ICPMS and determination of the isotope ratio pool available for plants from soil. *Anal. Bioanal. Chem.* **2010**, *398* (7−8), 3115−25.

(36) Moeller, K.; Schoenberg, R.; Pedersen, R.; Weiss, D. J.; Dong, S. Calibration of the new certified isotopic reference materials ERM-AE647 (Cu) and IRMM-3702 (Zn) against the previously used NIST SRM 976 (Cu) and 'JMC Lyon' (Zn) solutions − A new reference scale for copper and zinc isotope determinations. *Geostand. Geoanal. Res.* **2011**, *36*, 177−199.

(37) Bjerrum, J.; Schwarzenbach, G.; Sillen, L. G. *Stability Constants*; Chemical Society: London, 1958.

(38) Weiss, D. J.; Harris, C.; Maher, K.; Bullen, T. A Teaching Exercise To Introduce Stable Isotope Fractionation of Metals into Geochemistry Courses. *J. Chem. Educ.* **2013**, *90* (8), 1014−1017.

(39) Black, J. R.; Kavner, A.; Schauble, E. A. Calculation of equilibrium stable isotope partition function ratios for aqueous zinc complexes and metallic zinc. *Geochim. Cosmochim. Acta* **2011**, *75* (3), 769−783.

(40) Fujii, T.; Albarède, F., Ab initio calculation of the Zn isotope effect in phosphates, citrates, and malates and applications to plants and soil. *PLoS One* **2012**, *7*, (2), doi:e3072610.1371/journal.pone.0030726.

(41) Fujii, T.; Moynier, F.; Blichert-Toft, J.; Albarede, F. Density functional theory estimation of isotope fractionation of Fe, Ni, Cu and Zn among species relevant to geochemical and biological environments. *Geochim. Cosmochim. Acta* **2014**, *140*, 553−576.

(42) Moynier, F.; Fujii, T.; Wanga, K.; Foriel, J. Ab initio calculations of the Fe(II) and Fe(III) isotopic effects in citrates, nicotianamine,and phytosiderophore,and new Fe isotopic measurements in higher plants. *C. R. Geosci.* **2013**, *345*, 230.

(43) Domagal-Goldman, S. D.; Paul, K. W.; Sparks, D. L.; Kubicki, J. D. Quantum chemical study of the Fe(III)-desferrioxamine B siderophore complex—Electronic structure, vibrational frequencies, and equilibrium Fe-isotope fractionation. *Geochim. Cosmochim. Acta* **2009**, *73* (1), 1−12.

(44) Cloquet, C.; Carignan, J.; Lehmann, M. F.; Vanhaecke, F. Variations in the isotopic composition of zinc in the natural environment and the use of zinc isotopes in biogeosciences: a review. *Anal. Bioanal. Chem.* **2008**, *390*, 451−463.

(45) Little, S. H.; Vance, D.; Walker-Brown, C.; Landing, W. M. The oceaninc mass balance of copper and zinc isotopes, investigated by analysis of their inputs, and outputs to ferrommanganese oxide sediments. *Geochim. Cosmochim. Acta* **2014**, *125*, 673−693.

(46) Murakami, T.; Ise, K.; Hayakawa, M.; Kamei, S.; Takagi, S. Stabilities of metal complexes of mugineic acids and their specific affinities for iron(III). *Chem. Lett.* **1989**, *18*, 2137−2140.

(47) Brantley, S. L.; Liermann, L.; Bullen, T. D. Fractionation of Fe isotopes by soil microbes and organic acids. *Geology* **2001**, *29* (6), 535−538.

(48) Ptashnyk, M.; Roose, T.; Jones, D. L.; Kirk, G. J. D. Enhanced zinc uptake by rice by phytosiderophore secretion: a modelling study. *Plant, Cell Environ.* **2011**, *34* (12), 2038−2046.

(49) Smolders, E.; Versieren, L.; Dong, S.; Mattielli, N.; Weiss, D. J.; Petrov, I.; Degryse, F. Isotopic fractionation of Zn in tomato plants reveals the role of root exudates on Zn uptake. *Plant Soil* **2013**, *370* (1−2), 605−613.

(50) Caldelas, C.; Dong, S.; Araus, J. L.; Weiss, D. J. Zinc isotopic fractionation in *Phragmites australis* in response to toxic levels of zinc. *J. Exp. Bot.* **2011**, *62* (6), 2169−78.